ACADEMIC PRESS

Available online at www.sciencedirect.com
SCIENCE DIRECT®

Journal of Catalysis 218 (2003) 78–87

JOURNAL OF CATALYSIS

www.elsevier.com/locate/jcat

Alumina-supported molybdenum phosphide hydroprocessing catalysts

Paul A. Clark and S. Ted Oyama *

Environmental Catalysis and Materials Laboratory, Department of Chemical Engineering (0211), Virginia Polytechnic Institute and State University, Blacksburg, VA 24061, USA

Received 1 October 2002; revised 27 February 2003; accepted 27 February 2003

Abstract

Alumina-supported molybdenum phosphide hydroprocessing catalysts, MoP/γ-Al_2O_3, with weight loadings from 3.5 to 39 wt% were prepared by temperature-programmed reduction of alumina-supported molybdenum phosphate precursors. The precursors were obtained by incipient wetness impregnation of the support with aqueous molar solutions of ammonium paramolybdate and ammonium phosphate (Mo/P = 1/1). Effects of loading, reduction temperature, and heating rate on the catalysts were studied, and the samples were characterized by CO chemisorption, BET surface area, and X-ray diffraction (XRD) measurements. Compared to the bulk MoP and MoP/SiO_2 systems (which are similar to one another), the MoP/γ-Al_2O_3 material showed different behavior. Whereas calcined bulk and silica-supported molybdenum phosphates form Mo–P amorphous glasses which reduce directly to MoP, for the alumina-supported phosphates at high loadings (e.g., 13 wt% MoP/γ-Al_2O_3), a MoO_3 component is visible which reduces sequentially with temperature to MoO_2 and Mo metal, and then transforms to MoP. The difference in behavior between these systems is attributed to the formation of a strongly bound amorphous phosphate surface layer on the alumina support. Alumina has a strong affinity for phosphates, and appears to initially abstract a substantial amount of phosphorus from the stoichiometric molybdenum phosphate mixture. The alumina then releases the phosphorus at high temperature, allowing it to recombine with Mo metal to form MoP and generating active sites. The MoP/γ-Al_2O_3 catalysts performed well in hydroprocessing of a simulated distillate containing dibenzothiophene and quinoline at conditions representative of industrial hydroprocessing (643 K, 3.1 MPa). For the 13 wt% sample the hydrodesulfurization conversion was 57% and hydrodenitrogenation conversion was 62%. Catalytic activity, based on equal chemisorption sites loaded in the reactor (70 μmol), was generally independent of the amount of MoP deposited on the alumina surface, independent of the presence of X-ray visible molybdenum phases, and was associated with a relatively high temperature reduction peak found at all loading levels of MoP/Al_2O_3 but not in bulk MoP. We conclude that the high-temperature peak gives rise to highly dispersed MoP which is responsible for the bulk of the CO titration sites and the catalytic activity, and that the large MoP particles visible by XRD make smaller contributions.

Keywords: Molybdenum; Phosphide; Phosphorus; Alumina; Hydrodesulfurization; Hydrodenitrogenation; Dibenzothiophene; Quinoline

1. Introduction

Catalytic hydrotreating is an important refining process used to remove sulfur, nitrogen, and oxygen from hydrocarbon fuel liquids. Research in our laboratory has identified molybdenum phosphide, MoP, as an active and stable hydroprocessing catalyst [1–3]. Additional work by the group of Prins [4] has shown that MoP has six times higher activity in the HDN of orthopropylaniline than MoS_2/Al_2O_3. Studies in the group of Bussell have shown that MoP/SiO_2 has four times higher activity in the HDS of thiophene than MoS_2/Al_2O_3 [5]. In this paper we report the synthesis and catalytic properties of MoP deposited on a γ-alumina support.

MoP has a hexagonal WC-type structure, space group = $P_{6\tilde{m}2}$, with lattice parameters a_o = 322 pm and c_o = 319 pm [6]. MoP is a metallic conductor with properties similar to ordinary intermetallic compounds [7]. Fig. 1 shows the WC structure type adopted by MoP. The WC structure type, along with the NiAs and WP structures, characterize the majority of transition metal monophosphides. The WP structure type is similar to NiAs, but distortions in the (001) plane form a rectangular net, resulting in an orthorhombic structure [8]. A recent review summarizes the structure, preparation, and catalytic activity of phosphides [9].

Removal of heteroatoms from fuel liquids is important because sulfur and nitrogen compounds corrode engine com-

* Corresponding author.
E-mail address: oyama@vt.edu (S.T. Oyama).

0021-9517/03/$ – see front matter
doi:10.1016/S0021-9517(03)00086-1

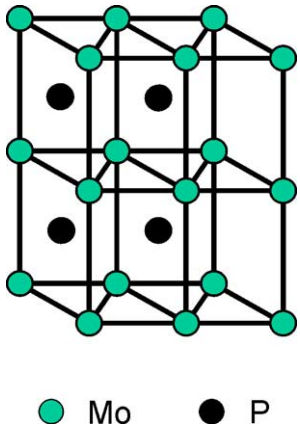

Fig. 1. Tungsten carbide (WC) structure type adopted by molybdenum phosphide, MoP.

ponents, pollute the air as SO_x and NO_x, cause gelling of untreated liquids, and foul downstream reforming catalysts. The problem is becoming increasingly important as government regulations become stricter [10] and the quality of petroleum feedstocks declines [11]. Although hydroprocessing catalysts have been widely studied, their basic compositions have changed little for many decades. They are typically alumina-supported molybdenum sulfides with nickel or cobalt promoters, $NiMoS/Al_2O_3$ or $CoMoS/Al_2O_3$ [12]. The catalysts described in this work are completely different, consisting of a compound of Mo and P with metallic rather than insulating or semiconducting properties.

In recent years, phosphorus has come to be used as a secondary promoter in commercial catalysts [13]. The use of phosphorus in hydroprocessing catalyst formulations was introduced in a series of patents dating back to the 1950s [14–16]. The phosphorus in these catalysts is dispersed on the catalyst surface in oxidized form, as shown by studies with X-ray photoelectron spectroscopy [17], nuclear magnetic resonance [18], and infrared spectroscopy [19]. The effect of phosphorus depends on its concentration and physical form, but in general it has a larger positive effect on the HDN performance of Ni–Mo sulfides than in the HDS performance of Co–Mo sulfide catalysts [20].

2. Experimental

Catalysts were prepared by impregnation and reduction. Desired quantities of ammonium paramolybdate tetrahydrate, $(NH_4)_6Mo_7O_{24}\cdot 4H_2O$ (Aldrich, 99%), and ammonium phosphate, $(NH_4)_2HPO_4$ (Aldrich, 99%), were dissolved in 1:1 stoichiometric proportions of metal to phosphorus to form clear solutions in distilled water. These solutions were used to fill the pores of a γ-alumina support (Degussa, Aluminumoxid C) by incipient wetness impregnation. The moist paste was calcined in air at 773 K for 6 h, ground with a mortar and pestle, pressed, broken, and sieved to particles between 650 and 1180 μm in diameter for use (mesh size 14/20). Samples were prepared with loadings between 0 and 39 wt% MoP (0 and 3.8 mmol g^{-1} Al_2O_3). Specific compositional characteristics for the series of catalysts are reported in Table 1. The highest loading sample was prepared by double impregnation, due to solubility limitations of the metal and phosphate salts in distilled water. Much of this study used the 13 wt% (1.16 mmol MoP g^{-1} Al_2O_3) MoP/Al_2O_3 material. Reference samples containing only 1.16 mmol Mo g^{-1} Al_2O_3 (10.0 wt% Mo) or 1.16 mmol P g^{-1} Al_2O_3 (3.5 wt% P) were prepared in a similar manner to the catalysts, while aluminum phosphate, $AlPO_4$, was purchased from a commercial source (Alfa-Aesar Division of Johnson-Matthey, 99.999%).

Table 1
Compositional characteristics of MoP/Al_2O_3 samples

wt% MoP	mmol MoP g^{-1} Al_2O_3	Molecules MoP nm^{-2} Al_2O_3
3.5	0.29	1.9
6.8	0.58	3.8
13	1.16	7.7
23	2.3	15
39	3.8	25

Temperature-programmed reductions were carried out on pelletized catalyst samples (typically 0.3 g) placed in quartz u-tube reactors. The samples were heated with linear temperature ramps in flowing hydrogen (Airco, 99.999%) to reduce the metal phosphate to metal phosphide. Unless otherwise noted, the space velocity was set at 650 μmol H_2 s^{-1} g^{-1} of sample loaded (1000 cm^3 (NTP) min^{-1} g^{-1}), and the heating rate was 0.0833 K s^{-1} (5 K min^{-1}). The effluent was monitored continuously by a mass spectrometer (Ametek/Dycor, MA100). All samples were flushed in hydrogen flow for 2 h before starting the temperature program, to dry the sample and to provide a starting baseline in the mass spectrometer. After reduction, the product was cooled to room temperature (RT) under helium (Airco, 99.999%) flow, and passivated progressively with 0.1% O_2/He, 0.5% O_2/He (Airco), and slow diffusion of air to the sample for 24 h.

The total dynamic CO uptake (Air Products, 99.999%) was measured with a mass spectrometer by passing 5.6 μmol pulses over the sample in 65 μmol s^{-1} helium flow at RT until constant area peaks were obtained. Measurements made on freshly reduced samples are referred to here as in situ CO uptakes while measurements taken on passivated samples rereduced in H_2 for 2 h at 723 K are referred to here as ex situ CO uptakes. BET specific surface areas (S_g) of passivated samples were measured with a Micromeritics 2000 sorption unit.

X-ray diffraction (XRD) patterns were obtained at a scan rate of 0.035° 2θ s^{-1} using a Scintag XDS-2000 diffractometer with a Ni-filtered Cu-K_α ($\lambda = 0.1541$ nm) radiation source. Crystallite sizes were estimated using the equation of Scherrer, $D = K\lambda/\beta\cos\theta$. The constant K was taken here to be 0.9, λ is the wavelength of radiation, β is the peak width in radians, and θ is the angle of the reflection. The

average of the first three reflections in MoP was used to calculate an average particle diameter [21]. Activation energies for reduction reactions were estimated by the heating rate variation method of Redhead [22].

Hydrotreating activity was evaluated with a model distillate containing 2000 wppm N as quinoline (Aldrich, 99%), 500 wppm O as benzofuran (Aldrich, 99%), 3000 wppm S as dibenzothiophene (Aldrich, 99%), 20 wt% tetralin (Aldrich, 99%), and balance tetradecane (Fisher, 99%). The catalytic test was carried out in an upflow, three-phase, fixed-bed reactor as described earlier [23]. An amount of catalyst corresponding to 70 μmol of CO sites (measured ex situ) was loaded for each reaction. To start the reaction, catalysts were pretreated in flowing hydrogen (100 $\mu mol\,s^{-1}$) at 723 K and 1 atm pressure for 2 h. The pressure was then increased to 3.1 MPa (450 psig), the temperature was dropped to 643 K (370 °C), and a liquid feed rate of 5 $cm^3\,min^{-1}$ (delivering 9.7 $\mu mol\,min^{-1}$ of quinoline and 6.3 $\mu mol\,min^{-1}$ of dibenzothiophene) was initiated. Analysis of hydroprocessing liquids was performed with a gas chromatograph (Hewlett-Packard, 5890A) on samples collected at 2- to 3-h intervals for a time period of 60–80 h, until a stable steady state was reached. In this report, hydrodesulfurization (HDS) is defined as the percentage disappearance of dibenzothiophene (as no sulfur-containing intermediates were observed), hydrogenation (HYD) is defined as the percentage of original quinoline converted to hydrogenated quinolines, and hydrodenitrogenation (HDN) is defined as the percentage of nitrogen removed from the quinoline delivered to the catalyst.

3. Results and discussion

3.1. Synthesis of MoP/γ-Al_2O_3

Calcined catalyst precursors were reduced to MoP/Al_2O_3 catalysts by temperature-programmed reduction in hydrogen at 0.0833 $K\,s^{-1}$ (5 $K\,min^{-1}$). Corresponding reduction profiles for 0–23 wt% MoP/Al_2O_3 samples are presented in Fig. 2. Five water peaks evolved through the reduction process, corresponding to reduction of different materials present in the precursor and to different stages in the reduction process. All of the samples, including the alumina support, exhibited a peak at 370 K (with a shoulder at 410–450 K) arising from physically adsorbed water. The alumina support alone exhibited no significant features above 500 K, while the molybdenum phosphate-loaded samples had features corresponding to reduction of the deposited species. These features were labeled α, β, γ, and δ in order of their appearance with temperature. The α peak occurred at the lowest temperatures, was relatively small, and was present in all of the samples. The δ peak was also present in all of the samples, occurred at the highest temperatures, and was generally large and diffuse. In the lowest loading materials, 3.5 and 6.8 wt%, the α and δ peaks constituted the majority of the reduction profile, and are attributed to well-dispersed

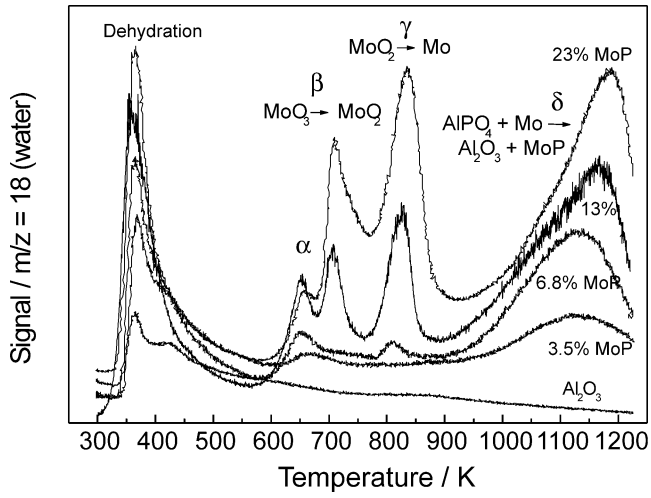

Fig. 2. Temperature programmed reduction profiles for various $MoPO_x/Al_2O_3$ samples reduced to 1223 K at 0.083 $K\,s^{-1}$ (5 $K\,min^{-1}$).

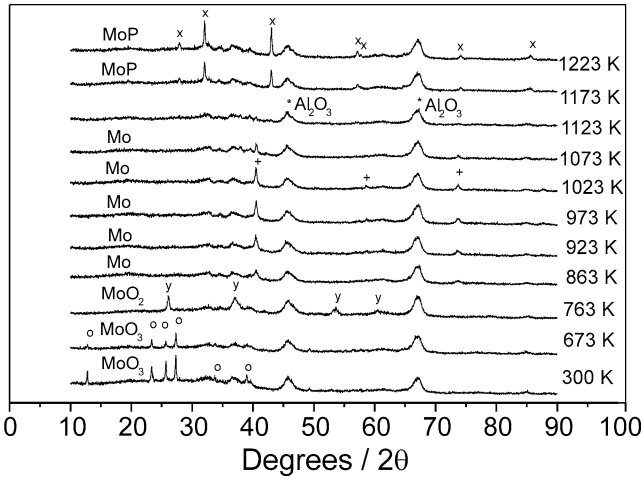

Fig. 3. Evolution of MoP during the reduction of $MoPO_x/Al_2O_3$ (13 wt% MoP). Samples were reduced to intermediate temperatures, quenched in helium, and characterized by in situ CO uptake before passivation. (○) MoO_3; (y) MoO_2; (+) Mo°; (×) MoP, and (∗) Al_2O_3.

species on the alumina surface. The γ peak first appeared as a small feature in the 6.8 wt% material, and was prevalent at higher loadings along with the β peak. The β and γ features slightly overlapped the α and δ features. But the β and γ peak temperatures were in the range typically observed for the reduction of bulk molybdenum compounds, and will presently be shown to correspond to X-ray visible phase changes.

The reduction of the 13 wt% MoP/Al_2O_3 material was followed by XRD of quenched and passivated intermediates. These spectra are shown in Fig. 3. Comparison of Fig. 2 with Fig. 3 allows association of the reduction peaks α, β, γ, and δ with phase changes observed by X-ray diffraction. The alumina-supported MoP precursor differs from the X-ray amorphous precursors for unsupported MoP [1] or silica-supported MoP [3] because of the visibility of MoO_3. The formation of MoO_3 is attributed to abstraction of the

phosphate component by the alumina surface. The take up of phosphate by alumina in standard phosphorus-promoted catalysts is well established [24,25].

The α peak near 675 K resulted in no new features in the XRD spectrum, and was therefore attributed to dehydroxylation of well-dispersed molybdate species. The low temperature of this feature is thought to arise because the strength of the alumina–molybdate bonds weakens the remaining hydroxyl bonds, which are subsequently easier to remove.

The β peak and γ peaks correspond to the transformation of MoO_3 to Mo metal through the intermediate MoO_2. This behavior is typical of the reduction of bulk MoO_3 in hydrogen. This X-ray observable process must occur because the phosphorus species are unavailable to the free molybdenum species. This demonstrates that the alumina fully binds the phosphate at this concentration level (13 wt% MoP). At higher surface loadings, the phosphate groups saturated the alumina surface and become available to associate with the free MoO_3. Here, the β and γ peaks resulted in XRD changes similar to substoichiometric MoP_xO_y ($x < 1$) oxides, where the value of x depends on the relative amount of P and Mo. Fortunately for the context of this report, catalysts prepared at 1123 K contained only MoP in their X-ray patterns (regenerated in the δ peak at higher temperatures), and the catalytic activity was attributed to well-dispersed phases not observed by XRD. Therefore, detailed characterization of the phase behavior of the samples with loading 23 and 38 wt% at intermediate temperatures was unnecessary.

Fig. 3 shows that the δ peak is accompanied by the disappearance of molybdenum metal and the appearance of molybdenum phosphide above 1123 K. This demonstrates that the δ peak is associated with the freeing of phosphorus within the sample, and its return to the molybdenum species. Indirectly, this shows that the δ peak is associated with reduction of alumina-bound phosphate groups, and indicates that phosphorus has a relatively fast diffusivity in molybdenum—because the freed phosphorus can penetrate the molybdenum metal completely to form pure MoP.

Fig. 4 shows the development of the in situ CO uptake in intermediates from the reduction of 13 wt% MoP/Al_2O_3 superimposed on its reduction profile. The CO uptake correlates reasonably well with the degree of completion of the reduction process, in which the dip at the end is likely due to sintering/grain growth of particles of the active phase due to the high temperature at that stage.

Table 2 summarizes the CO uptakes obtained for the 13 wt% sample at the different stages of reduction marked by peaks α, β, γ, and δ. It can be seen that the majority of the uptake is generated following the δ peak. Since the δ peak is also the major reduction peak in the low loading sample which does not show an X-ray visible MoP phase, this result suggests that the measured CO uptake in all the samples is associated with well-dispersed molybdenum phosphide held tightly on the alumina surface, rather than the X-ray visible phases.

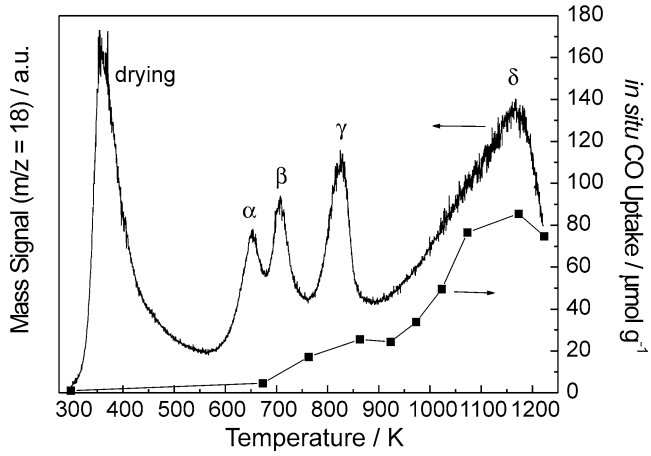

Fig. 4. Evolution of in situ CO uptake sites of quenched intermediates during the preparation of 13 wt% MoP/Al_2O_3.

Table 2
Evolution of CO uptake with the reduction peaks α, β, γ, and δ

Peak event	Temperature interval, K	CO uptake, μmol/g, %	X-ray visible phase change
α	298–673	4	None
β	673–763	15	$MoO_3 \rightarrow MoO_2$
γ	763–863	10	$MoO_2 \rightarrow$ Mo metal
δ	863–1173	71	Mo metal $\rightarrow$ MoP

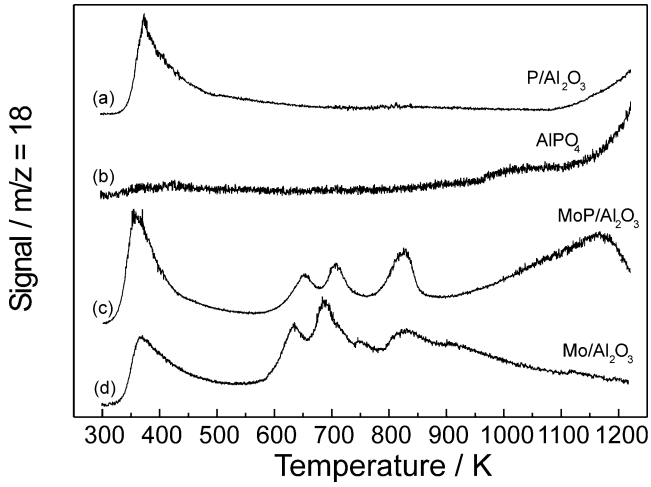

Fig. 5. Reduction profiles for "blank" alumina samples reduced to 1223 K at 0.083 K s^{-1} (5 K min^{-1}). (a) 1.16 mmol g^{-1} PO_x/Al_2O_3; (b) $AlPO_4$; (c) 1.16 mmol g^{-1} $MoPO_x/Al_2O_3$; and (d) 1.16 mmol g^{-1} MoO_x/Al_2O_3.

Fig. 5 shows reduction profiles of reference materials including commercial $AlPO_4$, the Al_2O_3 support containing only ammonium phosphate, and the Al_2O_3 support containing only ammonium molybdate. The supported reference materials were prepared with procedures (impregnation, calcination, and pelletization) and molar loading (1.16 mmol g^{-1} Al_2O_3) identical to those used for generating the 13 wt% MoP/Al_2O_3 catalyst. Samples containing the alumina support exhibited a large dehydration peak near 373 K. This low temperature behavior is sim-

ilar to that of the alumina blank and the supported catalysts shown in Fig. 2, and is attributed to the release of physically adsorbed water condensed in fine pores. Reference samples consisting of only P and Al_2O_3 had smooth baselines between 600 and 900 K, and developed peaks above 1100 K. A yellow-brown deposit formed downstream on the interior walls of the quartz reactor tube during the high-temperature peaks of the P and Al_2O_3 samples. The deposit is probably elemental phosphorus transported as volatile reduced species such as P_2, P_4, or PH_3 [26,27], but could be oxidized phosphorus transported as volatile P_2O_5. Vapor-phase transport of phosphorus has been reported earlier for phosphorus-containing materials undergoing high-temperature TPR [19]. The molybdenum-containing materials, Mo/Al_2O_3 and MoP/Al_2O_3, both had identifiable α, β, and γ peaks. These peaks are respectively attributed to recombination of hydroxyl ligands from well-dispersed molybdates, MoO_3 to MoO_2 reduction, and MoO_2 to Mo metal reduction. The Mo/Al_2O_3 had a tail above 900 K, attributed to the reduction of strongly held molybdates. In contrast to the reference samples, the MoP/Al_2O_3 sample had a large feature, the δ peak, between 900 and 1200 K. This feature in this temperature range only occurred in the presence of both phosphorus and molybdenum. X-ray diffraction indicated a phase change from Mo to MoP accompanying the δ peak, demonstrating influx of phosphorus from a source outside the molybdenum grains. The δ peak in the MoP/Al_2O_3 samples included the reduction of aluminum phosphate above 1100 K, but with the reduction temperature of phosphorus decreased because of facilitation of the reduction process by molybdenum.

X-ray diffraction spectra showing the presence of MoP in samples of different loading reduced to 1223 K at 0.0833 K s^{-1} (5 K min^{-1}) are presented in Fig. 6. MoP was the only crystalline product observed, becoming visible at 6.8 wt%, and increasing in intensity with loading. The XRD spectra of the catalysts reduced to 1123 K at 0.0833 K s^{-1} (5 K min^{-1}) and held for 2 h were similar to those shown in Fig. 6. The lattice constants of the supported MoP catalysts are reported in Table 3. The lattice parameters of the MoP in the catalysts agree well with the literature values, indicating that supported MoP of good purity is formed.

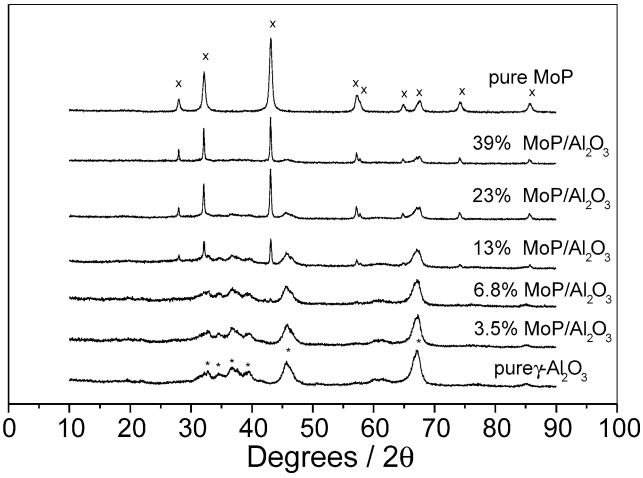

Fig. 6. X-ray diffraction results showing increased amounts of MoP with loading for samples reduced to 1223 K at 0.083 K s^{-1} (5 K min^{-1}). (×) MoP, and (∗) Al_2O_3.

The effect of final reduction temperature (heating rate $\beta = 5$ K min^{-1}) on catalytic performance was evaluated for the 13 wt% MoP/Al_2O_3 material. Of four temperatures investigated, successful samples were produced only at 1023 and 1123 K. Here, the primary criterion for success was the presence of sufficient and stable CO uptake for catalytic testing. A sample reduced at 873 K for 2 h had insufficient ex situ CO uptake (= 12 μmol g^{-1}) to load 70 μmol of sites, and a sample reduced at 1223 K for 0.5 h exhibited significant daily decrease in its CO uptake (noticed because of the averaging procedure used for catalyst samples) and was therefore also not used. Although the sample prepared at 1023 K had adequate CO uptake, its XRD spectrum revealed the presence of both Mo metal and MoP, while the sample reduced at 1123 K contained only MoP. Because of this, most of the supported samples used for the characterization and reactivity studies were reduced at 1123 K.

Table 3 summarizes crystallite sizes of the molybdenum phosphide calculated using the Scherrer equation. These values correspond to an average over the low index (1000), (1010), and (0001) planes. The sizes of the alumina-supported MoP crystallites increased slightly with the loading amount. More dramatic, however, was their large size (about double) compared to the bulk material. This is attributed to grain growth (Ostwald ripening or sintering) of the crystallites at the 200 K higher temperature of 1123 K used in the preparation of the supported catalysts compared to the bulk material, which was prepared with a maximum temperature of 923 K.

Table 3 also reports site densities of surface metal atoms calculated from the crystallite sizes of the X-ray visible MoP and the wt% loading of the MoP in the sample. The calculations were performed assuming spherical or cubic particles having surface site densities equal to 9.71 atoms nm^{-2}. It is understood that the crystallite size as given by the Scherrer

Table 3
X-ray diffraction results for MoP/Al_2O_3 catalysts

Sample	Lattice parameter, a_o (pm)	Lattice parameter, c_o (pm)	Crystallite size,[a] nm	Total metal site density,[b] μmol g^{-1}
13% MoP/Al_2O_3	321	318	39	43
23% MoP/Al_2O_3	322	319	40	75
39% MoP/Al_2O_3	322	319	51	98
MoP	322	318	19	680
MoP reference[c]	322	319	–	–

[a] Average size calculated from line broadening in the ⟨1000⟩, ⟨1010⟩, and ⟨0001⟩ directions.

[b] Site density = surface metal atoms per gram of sample. Calculated using the surface metal areal density of MoP (9.7×10^{18} surface Mo m^{-2}), the MoP fractional weight loading, and the average MoP crystallite size.

[c] JCPDS-ICDD Powder Diffraction File 24-771.

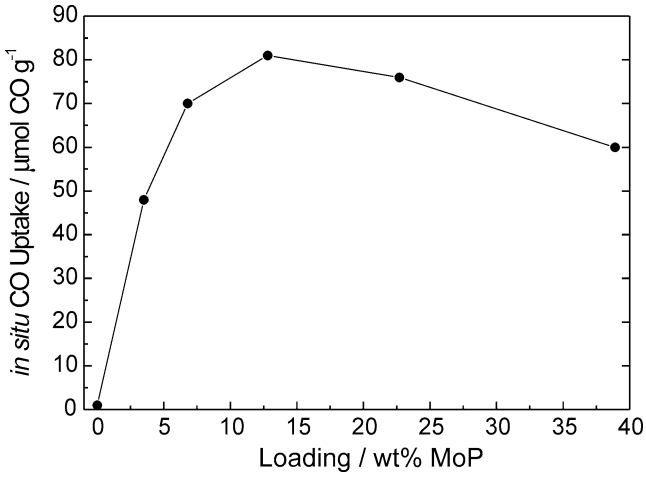

Fig. 7. Development of in situ CO uptake as a function of loading. The samples were reduced to 1223 K at 5 K min^{-1} in hydrogen flow at 670 μmol s^{-1} g^{-1} (1000 cm^3 min^{-1} g^{-1}).

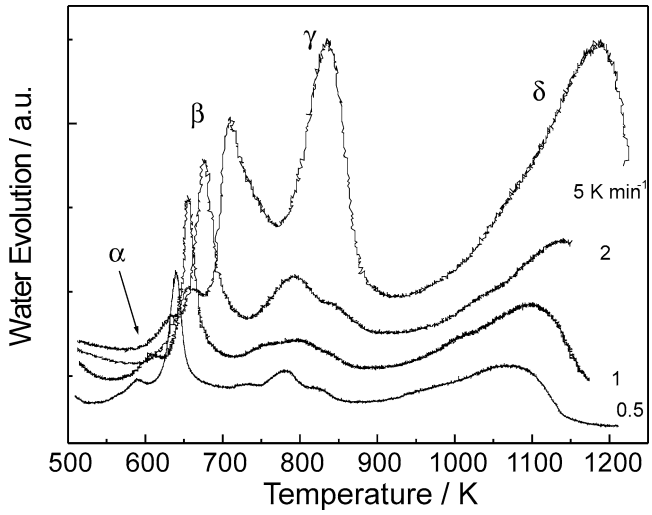

Fig. 8. Effect of heating rate on the temperature-programmed reduction forming 23 wt% MoP/Al_2O_3.

Table 4
Results of BET surface area and CO chemisorption measurements on MoP/Al_2O_3 samples

Sample	Surface area fresh,[c] m^2 g^{-1}	In situ[a] CO uptake, μmol g^{-1}	Ex situ[b] CO uptake fresh,[c] μmol g^{-1}	Ex situ[b] CO uptake spent,[d] μmol g^{-1}
γ-Al_2O_3	91[a]	1	0	–
6.8 wt% MoP	75	70	26	20
13 wt% MoP	71	81	36	31
23 wt% MoP	60	76	28	29
39 wt% MoP	49	60	36	26

[a] Samples reduced to 1223 K ($\beta = 5$ K min^{-1}, H_2 flow = 650 μmol g^{-1}) and then quenched.

[b] Pretreated in H_2 at 723 K for 2 h ($\beta = 5$ K min^{-1}, H_2 flow = 650 μmol g^{-1}).

[c] Catalysts prepared by reduction to 1123 K for 2 h ($\beta = 5$ K min^{-1}, H_2 flow = 650 μmol g^{-1}).

[d] Spent catalysts washed in hexane and dried in air.

Table 5
Apparent first-order activation energies of reduction events in the preparation of 23 wt% MoP/Al_2O_3

Peak	Activation energy, kJ mol^{-1}
α	152
β	157
γ	130*
δ	160

* Nonlinear. Estimated using heating rates of 2 K and 5 K min^{-1}. See text.

equation is only an approximation and ignores the presence of a distribution of sizes. The surface site density was calculated from the crystal structure of MoP [4] assuming exposure of equal numbers of low index planes. It is assumed in these calculations that the surface area to volume ratio of the MoP crystallites was proportional to 6/d (spherical or cube shaped particles), and that the particles had the density of bulk MoP [8] (7.50 g cm^{-3}). The site density of the unsupported MoP was much larger than the experimentally determined CO uptake of 18 μmol g^{-1} [1]. This reveals that the surface sites on bulk MoP are blocked in a ratio near 38:1, similar to results found for WP [28]. The calculated site densities were lower for the supported materials than the bulk due to a combination of larger MoP particles sizes and lower MoP weight fraction in the mixture.

Table 4 summarizes measurements of surface area, in situ CO uptake, and ex situ CO uptake for MoP/Al_2O_3 samples. The in situ CO uptakes were collected on the series of samples whose XRD spectra were presented in Fig. 6 and are plotted in Fig. 7. The in situ CO uptakes rose from 1 to 81 μmol per gram of sample as loading increased from 0 to 13 wt% MoP and then tapered off to 60 μmol per gram as loading was further increased to 39 wt%. The decrease at high loadings is likely due to blocking of pores by phosphide particles and consequent loss of surface area. Because the ex situ CO uptake of the fresh catalyst was used as the basis for loading the hydroprocessing reactor, these values were averaged over three measurements. The ex situ measurements on all of the catalyst samples were similar, regardless of loading, and the results on the fresh and spent catalysts show that the catalytic treatment led to only minor, if any, reductions in the ex situ CO uptake. Comparison of in situ and ex situ CO uptakes reveals that only a portion of the uptake sites are recovered after air exposure and subsequent rereduction.

Heating-rate variation between 0.5 and 5 K min^{-1} was investigated on the sample containing 2.3 mmol g^{-1} Al_2O_3 (23 wt% MoP/Al_2O_3). The reduction profiles are displayed in Fig. 8, and Table 5 reports the first-order activation energies calculated for each type of peak. As heating rate decreased, the relative intensity of the β peak increased, and the γ peak resolved into three smaller peaks. Furthermore, the γ peak maxima did not conform to a linear activation energy relationship. This behavior is consistent with satura-

tion of phosphorus on the alumina surface between 13 and 23 wt%, and the overlap of $MoO_2 \rightarrow Mo$ and $MoP_xO_y \rightarrow MoP_x$ processes in the γ peak. The origin of increased intensity of the β peak is not clear, but could be related to deeper reduction of the crystallites in the slower process.

3.2. Catalytic activity of MoP/γ-Al_2O_3 samples

The catalysts were evaluated for activity in hydrotreating of a simulated distillate containing quinoline (2000 wppm N) and dibenzothiophene (3000 wppm S) at 643 K and 3.1 MPa. Importantly, catalysts were loaded into the reactor using a constant 70 µmol ex situ CO uptake basis. The choice of ex situ CO uptake as the basis for comparison assumes catalytic activity to be due to surface sites generated through reduction at 723 K, and will be discussed later. The use of ex situ uptakes collected of air-exposed samples ensures that the sites are regenerated during catalytic pretreatment. Table 4 summarizes CO uptakes obtained after pretreatment in hydrogen at 723 K for 2 h.

Reference materials were also investigated for catalytic performance. These standards included the reduced support alone, a calcined phosphate blank containing 1.16 mmol PO_x g^{-1} Al_2O_3, and the phosphate blank exposed to the reduction procedure used for the majority of MoP/Al_2O_3 samples (1123 K for 2 h). An amount of 3.0 g of each blank was loaded, as their CO uptakes were negligible.

The hydrotreating performances of the samples are reported in Table 6. The blank reference materials had very low HDN and HDS conversions, as expected. For the MoP/Al_2O_3 samples there was only a minor effect of loading on the HDN and HDS performances, which averaged 56 and 52%, respectively. The amount of hydrogenated quinoline products was stable near 30% (except the phosphorus-containing blanks), consistent with equilibration between quinoline and 1,2,3,4-tetrahydroquinoline. Overall, the results indicate that a comparison of activity based on CO uptakes is reasonable. The single low HDS conversion of 44% for the 39 wt% sample is likely due to partial pore blockage for this high-loading sample. This would affect the larger dibenzothiophene more than the quinoline. The activity of the supported MoP/Al_2O_3 samples was moderately high, especially in HDN, and can be compared to that of a commercial Ni–Mo–S/Al_2O_3, which at the same hydroprocessing conditions had HDN conversion of 38% and HDS conversion of 79% [29].

Table 6
Hydroprocessing conversions of MoP/Al_2O_3 catalysts[a]

Sample	% HDN	% HYD	% HDS
Al_2O_3 blank	2.4	32	1.1
PO_x/Al_2O_3	3.3	18	4.7
P/Al_2O_3	3.8	19	1.0
6.8 wt% MoP	54	31	51
13 wt% MoP	52	33	57
13 wt% MoP[b]	62	29	57
23 wt% MoP	58	28	53
39 wt% MoP	54	33	44

[a] Reduced to 1123 K ($\beta = 5$ K min^{-1}, H_2 flow = 650 µmol g^{-1}) for 2 h.
[b] Reduced to 1023 K ($\beta = 5$ K min^{-1}, H_2 flow = 650 µmol g^{-1}) for 1.5 h.

Table 7 reports turnover frequencies (moles converted per CO uptake site per second) calculated for quinoline HDN and dibenzothiophene HDS for MoP supported on alumina compared with bulk MoP [1] and MoP on silica [3]. The silica-supported material shows somewhat lower activity when compared on this basis, and the alumina-supported material is similar to the bulk. This suggests that the MoP active sites formed on the alumina support are similar to the bulk material. Still the differences are small, and again indicate that CO uptakes are a reasonable method for comparing different samples.

Table 4 also reports the ex situ CO uptake values for the spent catalysts. For these measurements the samples were removed from the catalytic reactor, washed with hexane, and dried in air. Subsequently, they were reduced in hydrogen under the same conditions used for the fresh catalysts. The ex situ CO adsorption sites persisted following catalytic reaction conditions and exposure to air. This remarkable stability in CO uptake values before and after reaction is consistent with the stability in conversion levels noted for these catalysts.

X-ray diffraction traces for fresh and spent 13 wt% MoP/Al_2O_3 catalyst reduced to 1123 K are presented in Fig. 9. MoP and Al_2O_3 were the only crystalline phases observed, and the catalyst XRD signature was not significantly affected by the catalytic reaction. Similar results were found for catalysts of other loadings, whose XRD patterns were also stable toward the catalytic test, and which resembled the spectra shown in Fig. 6.

For the 13 wt% MoP/Al_2O_3 catalyst reduced at 1023 K (i.e., 100 K lower than the "standard" temperature of 1123 K), the X-ray diffraction patterns for the fresh and spent catalysts contained features of both Mo and MoP, as shown in Fig. 10. Nevertheless, this material was also active and stable toward the catalytic reaction conditions. This catalyst was prepared at 1023 K using a 1.5-h soak. Compared to the intermediate sample quenched at 1023 K, which contained only Mo metal in its XRD spectrum (Fig. 3), the diffraction trace of the catalyst sample reduced at 1023 K contained mostly MoP. Thus, the molybdenum phosphide in the catalyst sample appeared during the 1.5-h soak time en-

Table 7
Comparison of hydroprocessing turnover rates of 13% MoP/Al_2O_3 with 13% MoP/SiO_2 and bulk MoP

Sample	HDN, mol quinoline mol site^{-1} s^{-1}	HDS, mol dibenzothiophene mol site^{-1} s^{-1}
13 wt% MoP/Al_2O_3	1.2×10^{-3}	8.5×10^{-4}
13 wt% MoP/SiO_2	7.2×10^{-4}	3.0×10^{-4}
Bulk MoP	1.5×10^{-3}	5.2×10^{-4}

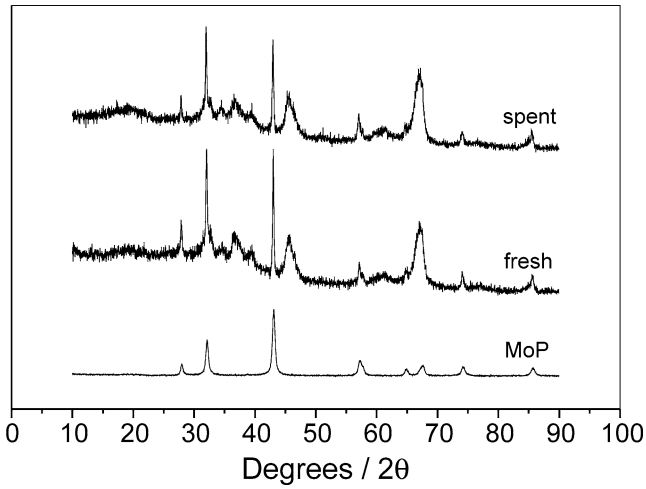

Fig. 9. X-ray diffraction of fresh and spent 13 wt% MoP/Al_2O_3 catalyst prepared at 1123 K.

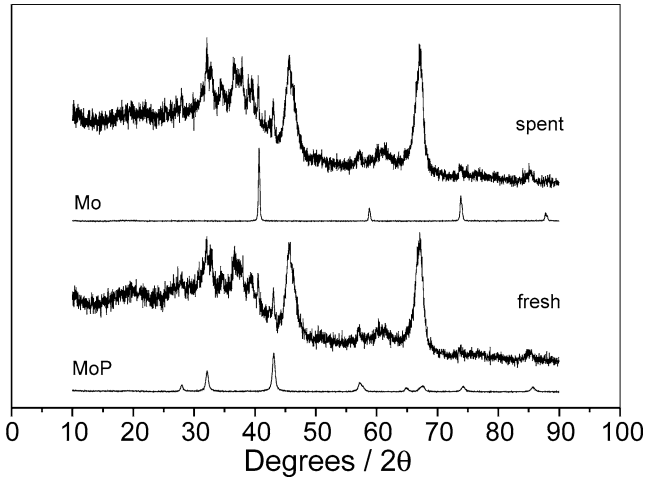

Fig. 10. X-ray diffraction of fresh and spent 13 wt% MoP/Al_2O_3 catalyst prepared at 1023 K.

tirely by the isothermal progress of the process giving the δ peak.

3.3. Nature of active sites

The choice of ex situ CO uptake as the basis of comparison of catalysts deserves commentary. Ordinarily for bulk materials, a surface area basis is chosen. However, in supported systems the surface area of the active phase and the support material combines and the relative surface of the active material is masked. By choosing a surface site titration technique (CO uptake) that is known to be roughly proportional to the total surface area [28], an estimate can be made of the amount of active surface available on a supported material. The CO uptake basis then allows comparisons of supported materials on the basis of equal active surface. While the correlation between CO uptake and catalytic performance is subject to experimental uncertainties, the relative correlation between CO uptake and catalytic activity (0.11 HDN, 0.25 HDS) in this study is substantially better than that found between catalytic activity and weight (0.32 HDN, 0.45 HDS), surface area (0.51 HDN, 0.33 HDS), or moles of molybdenum (1.33 HDN, 1.35 HDS). Here, the relative correlations represent variabilities, and are defined as the maximum span in values (maximum minus minimum) divided by the average value. For a previously undescribed catalyst system exhibiting a wide range of loadings and preparation conditions, we feel that the consistency of results based on CO uptakes is very good. Furthermore, the similarity of the turnover frequencies on CO uptake basis with bulk MoP is notable.

The majority of CO uptake in the MoP/Al_2O_3 system was generated by the δ reduction peak at much higher temperatures, about 200 K higher, than required for the formation of bulk MoP. The δ peak was observed in all of the MoP/Al_2O_3 samples, even at the lowest loading level of 3.2 wt%, and is attributed to highly dispersed molybdenum and phosphorus on the alumina surface. Our earlier EXAFS measurements [2] identified this dispersed phase in reduced 6.8 wt% MoP/Al_2O_3 to be clusters of MoP between 0.5 and 1.2 nm in size. The surface density (Table 1) of MoP on the 6.8 wt% sample is 3.8 MoP per nm^2, and appears to be slightly above the saturation limit of molybdenum on the alumina in this system (note the presence of traces of X-ray visible MoP in Fig. 6, and a slight gamma peak in Fig. 2). This saturation limit is slightly less than that of MoO_3, which forms a saturated monolayer on alumina at around 4.5 molecules/nm^2 [30]. Higher surface loadings of Mo and P up to 25 MoP/nm^2 (39 wt%) extend well beyond monolayer formation on the surface, and the excess molybdenum forms X-ray visible MoO_3 until phosphorus saturates as well, and substoichiometric molybdenum phosphate (MoP_xO_y, $x < 1$) species form at higher loadings. These X-ray visible excess molybdenum species undergo reduction in the temperature range of 650–850 K (at 5 K min^{-1}), as found in ordinary bulk Mo compounds, but the particles are generally very large. The relative sizes of the particles (Table 3) are much larger than bulk MoP produced at lower temperatures. The sizes of the particles and their dilution by alumina lead to much lower values of surface metallic densities than those found in bulk MoP. The relative similarity of turnover frequencies (Table 7) on the basis of CO uptake sites in alumina and bulk MoP materials indicates that the crystalline phases in the supported catalysts provide only a minimal contribution to the active surface in these materials.

Fig. 11 depicts a diagram of the proposed structure of the 6.8 wt% MoP/Al_2O_3 and 13 wt% MoP/Al_2O_3 materials. Here, the alumina particles and the associated oxide phases are highly simplified for the purpose of clarity. Nevertheless, the salient points of the process are clearly described. In the 6.8 wt% loading material, well-dispersed $MoPO_x$ reduces directly into MoP particles with diameters on the order of 1.2 nm. In the 13 wt% MoP material the precursor has distributed the molybdenum and phosphorus oxides as well dispersed $MoPO_x$, well dispersed aluminum phosphate,

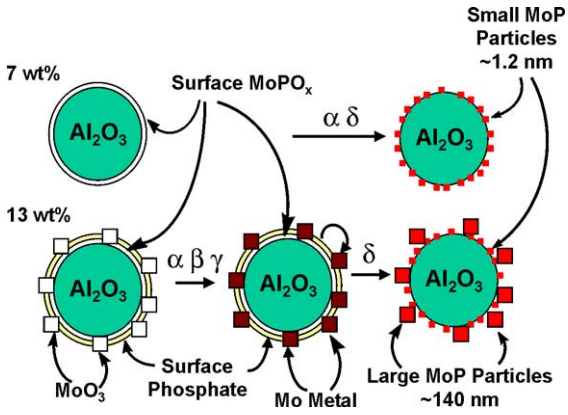

Fig. 11. Proposed structural model for 7 and 13 wt % MoP/Al_2O_3 catalysts.

and crystalline MoO_3. During the initial stages of reduction (i.e., the β and γ peaks), the crystalline MoO_3 reduces directly into metal, just as ordinary crystalline MoO_3 will do in the presence of hydrogen. During the latter stages of reduction (i.e., the δ peak), the dispersed aluminum phosphate is reduced to release phosphorus which is taken up by the molybdenum metal, and the well-dispersed $MoPO_x$ reduces directly into MoP particles with diameters on the order of 1.2 nm, as was found for the low loading sample.

3.4. Relationship to previous results in the literature

Although the nomenclature "MoP/Al_2O_3" has appeared before in the literature [31], the materials studied were in fact phosphate-promoted molybdenum sulfides. Such phosphate-promoted sulfidic hydrotreating catalysts have been widely investigated, as described in an extensive review by Iwamoto and Grimblot [13], but are not the same materials investigated in the present study. In our catalysts, the phosphorus is in a reduced state and the active molybdenum phosphide is metallic. Aside from the presence of Ni or Co promoters, comparison of the preparative conditions reveals that the relative amount of P to Mo in the promoted system is small, whereas in the present system it has exactly 1:1 molar proportions. For example, optimal activity for thiophene HDS in an alumina-supported sulfide catalyst containing 3.0 wt% NiO and 15 wt% MoO_3 was achieved with a phosphorus content of 1 wt% (0.24 mol P: mol Mo) [32]. Furthermore, the activation procedure for the promoted system typically involved low-temperature (ca. 723 K) reduction in a sulfidic atmosphere, whereas in the present study the reduction is at high temperature (1123 K) in pure hydrogen. No definitive evidence for phosphide formation has been given for the promoted system, whereas this study clearly demonstrates the presence of hexagonal MoP by XRD. Related work using EXAFS shows small crystallites containing Mo–P bonds [2].

There are also similarities between the phosphide and phosphorus-promoted sulfide systems. Both materials exhibit a strong interaction between phosphate and alumina [24,25]. Additionally, the presence of phosphate results in moderate reduction in the surface area of the catalysts. It has been found that the interaction of alumina and phosphate increases the dispersion of the metals in the Ni–Mo–S system [33]. Molybdena also interacts strongly with alumina, suggesting that the phosphate group alters the interaction of molybdenum with the surface [33].

Because the catalytic activity is roughly independent of loading from 6.8 to 39%, while the XRD of MoP increases dramatically in intensity, it is reasonable to conclude that the majority of active sites are associated with highly dispersed MoP clusters in close contact with Al_2O_3, as noted earlier [2]. The nature of phosphorus in MoP/Al_2O_3 catalysts reported here is quite different from its oxidized state in commercial phosphorus-promoted sulfides. The MoP/Al_2O_3 catalysts reported in this paper are reduced at substantially higher temperatures than those employed in standard sulfiding, and result in the reduction and transfer of phosphorus from alumina to the metallic phase. That the temperature of preparation is 200 K higher than for ordinary bulk MoP is also remarkable, because it reveals that the alumina support stabilizes very small MoP particles, protecting them from sintering and maintaining their surface sites.

4. Conclusions

A series of MoP catalysts supported on γ-Al_2O_3 was prepared and tested for hydroprocessing activity under simulated industrial conditions. MoP/Al_2O_3 catalysts were effective at HDN and HDS in our tests, averaging 57 and 52%, respectively. Interestingly, dispersion of the molybdenum phosphate precursor on alumina revealed substantially different phase behavior than found in bulk MoP and silica supported MoP. At loadings between 0 and $\sim$ 6 wt%, both the molybdenum and phosphorus species were distributed on the alumina support with a strong interaction. At about 6 wt%, the molybdenum species saturated on the alumina support and increases in surface loading led to free MoO_3 in the oxidized system. Above 13 wt%, the phosphorus also saturates on the alumina surface and further increases in surface loading produced combinations of MoO_3 and substoichiometric MoP_xO_y ($x < 1$) species. Regardless of the X-ray visible phases, catalytic activity was independent of loading and was attributed to well-dispersed MoP formed from the reduction of the first 6 wt% of molybdenum phosphate deposited to the surface.

Higher loadings also resulted in strong interaction between alumina and phosphate. Evidence for this was found in the presence of MoO_3 in the oxidic precursor form of the 13 wt% MoP/Al_2O_3 catalyst, and by new peaks in the TPR profile. As reduction proceeded, MoO_2 occurred at 763 K, molybdenum metal was seen between 863 and 1073 K, and MoP was formed above 1173 K. The catalysts were active for hydroprocessing of both dibenzothiophene and quinoline, and were stable under hydroprocessing conditions. Analysis suggests that the active sites are associated

with small (∼ 1.2 nm) phosphide crystallites on the alumina carrier surface.

Acknowledgments

This work was carried out with support from the United States Department of Energy, Office of Basic Energy Sciences, Grant DE-FG02-96ER14669. The authors thank Doo Hwan Lee for the surface area measurements.

References

[1] W. Li, B. Dhandapani, S.T. Oyama, Chem. Lett. (1998) 207.
[2] S.T. Oyama, P.A. Clark, V.L.S. Teixeira da Silva, E.J. Lede, F.G. Requejo, J. Phys. Chem. B 105 (2001) 4961.
[3] P.A. Clark, X. Wang, S.T. Oyama, J. Catal. 207 (2002) 256.
[4] C. Stinner, R. Prins, Th. Weber, J. Catal. 191 (2000) 438.
[5] D.C. Phillips, S.J. Sawhill, R. Self, M.E. Bussell, J. Catal. 208 (2002) 456.
[6] S. Rundqvist, T. Lundstrom, Acta Chem. Scand. 17 (1963) 37.
[7] S. Rundqvist, Colloq. Int. Centre Nat. Rech. Sci. 157 (1967) 85.
[8] N. Schönberg, Acta Chem. Scand. 8 (1954) 226.
[9] S.T. Oyama, J. Catal. (2003), in press.
[10] Chem. Eng. News May 22 (2000) 27.
[11] J.W.M. Sonnemans, Stud. Surf. Sci. Catal. 100 (1995) 99.
[12] H. Topsøe, B.S. Clausen, F.E. Massoth, Hydrotreating Catalysis-Science and Technology, Springer, Berlin, 1996.
[13] R. Iwamoto, J. Grimblot, Adv. Cat. 44 (1999) 417.
[14] J.N. Haresnape, J.E. Morris, British patent 701217, 1953.
[15] E.C. Housam, R. Lester, British patent 807583, 1959.
[16] G.A. Mickelson, US patents 3749663, 3755196, 3755150, 3755148, and 3749664, 1973.
[17] D. Chadwick, D.W. Aitchison, R. Badilla-Ohlbaum, L. Josefson, Stud. Surf. Sci. Catal. 16 (1983) 323.
[18] A.N. Startsev, O.V. Klimov, A.V. Kalinkin, V.M. Mastikhin, Kinet. Catal. 35 (1994) 552.
[19] P.J. Mangnus, J.A.R. van Veen, S. Eijsbouts, V.H.J. de Beer, J.A. Moulijn, Appl. Catal. 61 (1990) 99.
[20] P. Atanasova, T. Tabakova, Ch. Vladov, T. Halachov, A. Lopez Agudo, Appl. Catal. A 161 (1997) 105.
[21] B.D. Cullity, Elements of X-Ray Diffraction, 2nd ed., Addison–Wesley, Menlo Park, CA, 1978, p. 102.
[22] J.L. Falconer, J.A. Schwarz, Catal. Rev. Sci. Eng. 25 (1983) 141.
[23] S. Ramanathan, S.T. Oyama, J. Phys. Chem. 99 (1995) 16365.
[24] J.A.R. van Veen, P.A.J.M. Handriks, E.J.G.M. Romers, R.R. Andréa, J. Phys. Chem. 94 (1990) 5282.
[25] S.M.A.M. Beuwens, J.P.R. Vissers, V.H.J. de Beer, R. Prins, J. Catal. 112 (1988) 401.
[26] J.R. van Wazer, Phosphorus and Its Compounds, Interscience, New York, 1958, Vol. 1.
[27] K.A. Gingerich, J. Phys. Chem. 68 (1964) 2514.
[28] P. Clark, W. Li, S.T. Oyama, J. Catal. 200 (2001) 140.
[29] B. Dhandapani, S. Ramanathan, C.C. Yu, B. Fruhberger, J.G. Chen, S.T. Oyama, J. Catal. 176 (1998) 61.
[30] U.S. Ozkan, L. Zhang, S. Ni, E. Moctezuma, J. Catal. 148 (1994) 181.
[31] M. Jian, R. Prins, Bull. Soc. Chim. Belg. 104 (1995) 231.
[32] J.M. Lewis, R.A. Kydd, P.M. Boorman, P.H. van Rhyn, Appl. Catal. A 84 (1992) 103.
[33] P. Atanasova, R. López-Cordero, L. Mintchev, T. Halachev, A. López-Agudo, Appl. Catal. A 159 (1997) 269.